

1 KINETIC MODELING OF ELECTRO-FENTON REACTION IN AQUEOUS SOLUTION

2

3 H. Liu¹, X. Z. LI^{*2}, Y. J. Leng³, C. Wang¹4 ¹*School of Chemistry and Chemical Engineering, Sun Yat-sen University, Guangzhou, 510275,*
5 *China.*6 ²*Department of Civil and Structural Engineering, The Hong Kong Polytechnic University, Hong*
7 *Kong, China*8 ³*School of Mechanical and Aerospace Engineering, Nanyang Technological University, 50 Nanyang*
9 *Ave, Singapore 639798*

10

11 **Abstract**

12 To well describe the electro-Fenton (E-Fenton) reaction in aqueous solution, a new kinetic model
13 was established according to the generally-accepted mechanism of E-Fenton reaction. The model
14 has special consideration on the rates of hydrogen peroxide (H₂O₂) generation and consumption in
15 the reaction solution. The model also embraces three key operating factors affecting the organic
16 degradation in the E-Fenton reaction, including current density, dissolved oxygen concentration and
17 initial ferrous ion concentration. This analytical model was then validated by the experiments of
18 phenol degradation in aqueous solution. The experiments demonstrated that the H₂O₂ was gradually
19 built up with time and eventually approached its maximum value in the reaction solution. The
20 experiments also showed that phenol was degraded at a slow rate at the early stage of the reaction, a
21 faster rate during the middle stage, and a slow rate again at the final stage. It was confirmed in all
22 experiments that the curves of phenol degradation (concentration vs. time) appeared to be an
23 inverted “S” shape. The experimental data were fitted using both the normal first-order model and
24 our new model, respectively. The goodness of fittings demonstrated that the new model could better
25 fit the experimental data in all experiments than the first-order model appreciably, which indicates
26 that this analytical model can better describe the kinetics of the E-Fenton reaction mathematically
27 and also chemically.

28 *Keywords:* E-Fenton; H₂O₂; Kinetic Model; Phenol

* Corresponding author, Tel.: (852) 2766 6016; Fax: (852) 2334 6389; Email address: cexzli@polyu.edu.hk

29 **1. Introduction**

30

31 It has been well proven that a variety of refractory organics can be effectively degraded by the
32 Fenton reaction without producing any toxic substances in water environment (Joseph, 1992;
33 Oliveros et al., 1997; Lunar et al., 2000; Kawabe et al., 2004; Wang et al., 2004). Recent
34 development of electro-Fenton (E-Fenton) reaction by generating H_2O_2 from dissolved oxygen in
35 aqueous solution electrically provides fresh H_2O_2 in a continuous mode, which is more efficient and
36 cost-effective than conventional chemical dosing methods (Brillas et al., 1998; Brillas et al., 2000;
37 Brillas and Casado, 2002; Brillas et al., 2003; Gözmen et al., 2003).

38 It should be noted that like most chemical reactions, the H_2O_2 concentration in a conventional
39 Fenton reaction is gradually reduced after a batch chemical dosing along with reaction time (Malato
40 et al., 2001; Liu et al., 2003). It has been reported that adding H_2O_2 in a single batch leaves much of
41 it available to attack by hydroxyl radicals, whereas continuously feeding smaller quantities of the
42 reagent to the system would allow the majority of radicals generated to target the organic
43 contaminant (Duesterberg and Waite, 2006). In an E-Fenton reaction process, H_2O_2 is continuously
44 generated on the cathode throughout the reaction and its accumulative concentration in aqueous
45 solution depends on a competition between its generation rate and consumption rate (Oturán, 2000;
46 Oturán et al., 2000; Boye et al., 2002). Particularly, at the beginning of the reaction such as the first
47 5 min, the H_2O_2 concentration rises from zero and the rate of organic degradation in aqueous
48 solution is quite slow, although H_2O_2 concentration builds up at a maximum rate. When the reaction
49 further proceeds, the rate of organic degradation is gradually increased with the increased H_2O_2
50 concentration and then eventually decreased again. Therefore, the most commonly-used first-order
51 reaction model has a difficulty to well describe the kinetics with a continuous H_2O_2 supply,
52 particularly during the initial reaction period of the E-Fenton reaction (Malato et al., 2001; Gözmen
53 et al., 2003). Wang and Lemley in 2001 developed a second-order kinetic model to describe the
54 E-Fenton reaction (anodic Fenton reaction) for degradation of 2,4-dichlorophenoxyacetic acid in
55 aqueous solution as a more accurate kinetic model than the first-order model. Moreover, a recent
56 work by Anota et al. in 2006 compared the kinetics of aniline degradation by Fenton and E-Fenton
57 reactions. It was found that the overall rate equation for aniline degradation by Fenton reaction
58 followed a reaction order of 1.1 (almost a first-order reaction), but that by E-Fenton reaction

59 demonstrated a reaction order of 0.46 (about a half-order reaction). Alternatively, other researchers
60 still applied the first-order model to describe the E-Fenton reaction but either in terms of total
61 organic carbon (Brillas et al., 1998; Brillas et al., 2000) or by subdividing the overall reaction
62 period into two or three phases with different values of kinetic constant representing different
63 reaction rates (Chu et al., 2005). It should be indicated that a good kinetic model to well describe
64 the E-Fenton reaction should consider some other key factors including current density, dissolved
65 oxygen concentration and ferrous ion concentration jointly.

66 In this work, a new kinetic model for the E-Fenton reaction in aqueous solution was established
67 according to the generally-accepted mechanism of the E-Fenton reaction. Phenol was used as a
68 model pollutant and a series of phenol degradation experiments in an E-Fenton reaction system
69 were carried out. The new model was then validated by the experimental data and evaluated in this
70 study.

71

72 **2. Experimental Section**

73

74 *2.1. Chemicals*

75

76 Phenol, hydrogen peroxide (H_2O_2 , 30% w/v), sodium sulfate (Na_2SO_4), potassium titanium (IV)
77 oxalate [$\text{K}_2\text{Ti}(\text{C}_2\text{O}_4)_3$] and ferrous sulfate ($\text{FeSO}_4 \cdot 7\text{H}_2\text{O}$) chemicals were obtained from Aldrich,
78 USA with analytical grade and used without further purification.

79

80 *2.2. Experimental setup*

81

82 All experiments were conducted in an E-Fenton reactor consisting of two electrochemical cells
83 connected with a glass frit. A Pt flake (20 mm \times 20 mm) from Superior Chemicals & Instruments,
84 China was used as the anode and a commercially-available carbon rod ($\Phi = 5$ mm and $L = 80$ mm)
85 from Shanghai, China was employed as the cathode to generate H_2O_2 . In addition, a saturated
86 calomel electrode was applied as the reference electrode. Both the cathode and the reference
87 electrode are placed in one compartment, while the anode is placed in another compartment. A
88 potentiostat/galvanostat (ZF-9) from Zhenfang Electronic Ltd., China was employed to apply an

89 electrical current between the anode and cathode. This E-Fenton reactor has an effective volume of
90 150 mL. Phenol solution was prepared in aqueous 0.01 M Na₂SO₄ electrolyte solution. The pH of
91 reaction solution was adjusted to be 2.5 using 0.1 M H₂SO₄ before reaction. A mixture gas of
92 oxygen and air was continuously bubbled through a sintered-glass diffuser to supply dissolved
93 oxygen and also to provide mixing, in which the concentrations of dissolved oxygen in the reaction
94 solution were maintained at 0.26 mM, 0.40 mM and 0.57 mM, respectively in three sets of
95 experiments, when different ratios between oxygen and air gases were controlled. During the
96 reaction, water samples were collected at different time intervals for analyses. To quench any
97 further reaction with radicals in the samples, 10 μL of methanol was injected into the 2.0 mL of
98 sample as soon as the sample taking.

99

100 *2.3. Analytical Methods*

101

102 Phenol concentration was analyzed by HPLC (Waters 486) equipped with a reverse-phase column
103 (Waters, XTerra™ MS C-18) and a UV detector. A mobile phase consists of acetonitrile and water
104 (20%:80%) with 0.5% acetic acid. Under these conditions, phenol was determined at the
105 wavelength of 269 nm with a retention time of 5.8 min. The ferrous ion (Fe²⁺) concentration was
106 determined using a UV-VIS spectrophotometer (Spectronic, GENISIS-2), according to the light
107 absorption at 510 nm of a colored complex solution formed from Fe²⁺ and 1,10-phenanthroline
108 (APHA, 1995). H₂O₂ solution was prepared with 30% H₂O₂ chemical and calibrated by KMnO₄
109 titration, which had been calibrated by Na₂C₂O₄ titration (Vogel, 1978). Whereas, the H₂O₂
110 concentration during the E-Fenton reaction was determined using the UV-VIS spectrophotometer,
111 according to the light absorption at 407 nm of a yellow complex solution formed from the H₂O₂ and
112 K₂Ti(C₂O₄)₃ in 2 M H₂SO₄ solution to prevent any interference caused by the organic disturbance
113 (Sellers, 1980).

114

115 **3. Kinetic Modeling of E-Fenton Reaction**

116

117 It is generally believed that a typical E-Fenton reaction should involve three key reactions: (1) the
118 generation of H₂O₂ from dissolved oxygen on the surface of the cathode (Reaction 1), (2) the

119 generation of hydroxyl radicals ($\cdot\text{OH}$) between H_2O_2 and Fe^{2+} (Reaction 2), and (3) the degradation
 120 of organic substance by the $\cdot\text{OH}$ (Reaction 5). In the meantime, some reversed reactions and side
 121 reactions (Reactions 3, 4, 6 and 7) coexist along with the key reactions as summarized below
 122 (Walling, 1975; Buvet et al., 1987; Neyens and Baeyens, 2003);



130 To establish a new kinetic model for describing the E-Fenton reaction, we may assume that
 131 organic substance (S) is primarily degraded by the $\cdot\text{OH}$ and its reaction rate ($\frac{d[S]}{dt}$) can be
 132 expressed by Eq. 1:

133
 134
$$-\frac{d[S]}{dt} = k_5[\cdot\text{OH}] \cdot [S] \quad (1)$$

135 From the reactions 2, 3, 5, and 7, the change of $\cdot\text{OH}$ concentration ($\frac{d[\cdot\text{OH}]}{dt}$) relies on its
 136 generation rate from H_2O_2 and Fe^{2+} , and its consumption rate reacting with Fe^{2+} , organic substance
 137 and H_2O_2 as shown below:

138
 139
$$\frac{d[\cdot\text{OH}]}{dt} = k_2[\text{Fe}^{2+}] \cdot [\text{H}_2\text{O}_2] - k_3[\text{Fe}^{2+}] \cdot [\cdot\text{OH}] - k_5[\cdot\text{OH}][S] - k_7[\cdot\text{OH}][\text{H}_2\text{O}_2] \quad (1a)$$

 140

141 Since k_7 (3.30×10^7) is about one order smaller than k_3 (3.20×10^8) at pH 3-4 according to the
 142 data in the literature (Dueterberg and Waite, 2006) and also $[\text{H}_2\text{O}_2]$ is much lower than $[\text{Fe}^{2+}]$ in
 143 our E-Fenton reaction system, it is fair enough to remove the item of $k_7[\cdot\text{OH}][\text{H}_2\text{O}_2]$ from Eq. 1a in
 144 order to simplify the model.

145 Also, since $\cdot\text{OH}$ is a highly-reactive free radical with an extremely-short lifetime of
 146 nanoseconds (Liu et al., 1999), its concentration is normally considered to be constant but at a low
 147 level and the $\frac{d[\cdot\text{OH}]}{dt}$ will approach zero according to a steady state approximation. Then Eq. 1 can
 148 be rearranged as Eq. 2 and the rate of organic degradation becomes a function of $[\text{H}_2\text{O}_2]$ and $[\text{S}]$
 149 mainly.

$$150 \quad -\frac{d[\text{S}]}{dt} = k_5 \cdot \frac{k_2[\text{Fe}^{2+}] \cdot [\text{S}]}{k_3[\text{Fe}^{2+}] + k_5[\text{S}]} \cdot [\text{H}_2\text{O}_2] \quad (2)$$

151 On the other hand, the variation of H_2O_2 concentration in the reaction solution depends on its
 152 generation rate (Reaction 1) and decomposition rate (Reactions 2, 4, 6 and 7). If it is assumed that
 153 the rate of H_2O_2 generation is proportional to the applied current density (I/A) and the oxygen
 154 coverage (θ) on the cathode, it can be expressed by Eq. 3.

$$155 \quad \frac{d[\text{H}_2\text{O}_2]}{dt} = k_1 \cdot \frac{I \cdot \theta}{A} - (k_2[\text{Fe}^{2+}] + k_4[\text{Fe}^{3+}]) \cdot [\text{H}_2\text{O}_2] - k_6[\text{H}_2\text{O}_2] \cdot [\text{S}] - k_7[\cdot\text{OH}] \cdot [\text{H}_2\text{O}_2] \quad (3)$$

156
 157 By considering that the adsorption of dissolved oxygen on the cathode surface obeys the
 158 Langmuir adsorption model, a relationship between oxygen coverage (θ) and dissolved oxygen
 159 concentration ($[\text{O}_2]$) can be expressed by the following equation, where K_{ad} is the adsorption
 160 equilibrium constant.
 161

$$162 \quad \theta = \frac{K_{ad}[\text{O}_2]}{1 + K_{ad}[\text{O}_2]}$$

163
 164 Since $k_2 \gg k_4, k_6$ and k_7 , Eq. 3 can be simplified into Eq. 4. After integration, the $[\text{H}_2\text{O}_2]$
 165 becomes a function of experimental time (t). According to the initial condition when $t = 0$, $[\text{H}_2\text{O}_2] =$
 166 0 , and also assuming that the $[\text{Fe}^{2+}]$ during the reaction is proportional to its initial concentration
 167 ($[\text{Fe}^{2+}]_0$) with a fixed ratio of λ , $[\text{H}_2\text{O}_2]$ can be eventually expressed as Eq. 5.
 168

$$169 \quad \frac{d[\text{H}_2\text{O}_2]}{dt} = k_1 \cdot \frac{Ik_{ad}[\text{O}_2]}{A(1 + k_{ad}[\text{O}_2])} - k_2[\text{Fe}^{2+}] \cdot [\text{H}_2\text{O}_2] \quad (4)$$

171

$$[H_2O_2] = \frac{k_1 K_{ad} I[O_2]}{k_2 \lambda A [Fe^{2+}]_0 (1 + K_{ad} [O_2])} (1 - e^{-k_2 \lambda [Fe^{2+}]_0 t}) \quad (5)$$

173

174 The above equation indicates that the $[H_2O_2]$ is a function of experimental time, increasing
 175 from zero at the beginning of reaction ($t = 0$) toward its maximum value after sufficient reaction
 176 time as shown below:

177

$$[H_2O_2]_{max} = \frac{k_1 K_{ad} I[O_2]}{k_2 \lambda A [Fe^{2+}]_0 (1 + K_{ad} [O_2])} \quad (5a)$$

179

180 This equation demonstrates that $[H_2O_2]_{max}$ in the E-Fenton reaction depends on few factors of
 181 I/A , $[Fe^{2+}]_0$ and $[O_2]$. Alternatively Eq. 5 has a simplified form as shown below:

182

$$[H_2O_2] = [H_2O_2]_{max} (1 - e^{-k_2 \lambda [Fe^{2+}]_0 t}) \quad (5b)$$

184

185 Once we use Eq. 5 to replace the $[H_2O_2]$ in Eq. 2, the rate of organic degradation can be further
 186 expressed as follows:

187

$$-\frac{d[S]}{dt} = \frac{k_5}{k_3 \lambda [Fe^{2+}]_0 + k_5 [S]} \cdot \frac{k_1 K_{ad} I[O_2]}{(1 + K_{ad} [O_2])} (1 - e^{-(k_2 \lambda [Fe^{2+}]_0)t}) \cdot [S] \quad (2a)$$

189

190 After integration, the organic concentration $[S]$ becomes a function of experimental time,
 191 decreasing from its initial concentration $[S]_0$ at the beginning of reaction ($t = 0$) gradually as
 192 described by Eq. 6:

193

$$Ln\left(\frac{[S_0]}{[S]}\right) + \frac{k_5}{k_3 \lambda [Fe^{2+}]_0} ([S_0] - [S]) = \frac{k_1 k_5 K_{ad} I[O_2]}{k_3 \lambda A [Fe^{2+}]_0 (1 + K_{ad} [O_2])} \left(t - \frac{1 - e^{-(k_2 \lambda [Fe^{2+}]_0)t}}{k_2 \lambda [Fe^{2+}]_0} \right) \quad (6)$$

195

196 To simplify Eq. 6, let $a = \frac{k_5}{k_3 \lambda [Fe^{2+}]_0}$, $b = \frac{k_1 k_5 K_{ad} I [O_2]}{k_3 \lambda A [Fe^{2+}]_0 (1 + K_{ad} [O_2])}$ and $c = k_2 \lambda [Fe^{2+}]_0$, the above equation
 197 can be re-arranged in a simplified form as shown below:

198

$$199 \quad \ln \frac{[S_0]}{[S]} + a([S_0] - [S]) = b \left(t - \frac{1 - e^{-ct}}{c} \right) \quad (6a)$$

200

201 It can be concluded that the above pair of equations (Eqs. 5 and 6) has been established as the
 202 main kinetic model for the E-Fenton reaction to describe H₂O₂ accumulation and organic
 203 degradation in aqueous solution against reaction time.

204

205 **4. Validation of the New Kinetic Model by Experiments**

206

207 To validate the new model for its application in an E-Fenton reaction system, three sets of
 208 experiments were carried out in aqueous phenol solution by varying three key factors of current
 209 density (I/A), dissolved oxygen concentration ([O₂]) and ferrous ion concentration ([Fe²⁺]),
 210 respectively. Each experiment with an initial phenol concentration of 1.5 × 10⁻⁴ M and initial pH 2.5
 211 lasted for up to 90 min, in which the concentrations of H₂O₂ and phenol were determined at
 212 different reaction intervals.

213 The H₂O₂ model (Eq. 5b) was first validated by the above experimental data of H₂O₂
 214 concentration. The fitting results are presented in Fig. 1. It can be seen clearly that the new H₂O₂
 215 model can well describe the H₂O₂ variation in all experiments. Both the experimental data and the
 216 model simulation showed that H₂O₂ concentration increased quickly at the initial stage of the
 217 reaction and gradually approached to the maximum values. The experimental results in Fig. 1A and
 218 B indicate that the higher I/A and [O₂] would be beneficial to enhance the H₂O₂ generation rate,
 219 while the results in Fig. 1C show that the higher [Fe²⁺] could decompose H₂O₂ faster. These
 220 experimental data were also fitted using Eq. 5 to demonstrate the relationship between [H₂O₂]_{max}
 221 and three factors of current density, dissolved oxygen concentration and initial ferrous ion
 222 concentration, respectively as shown in Fig. 2. The fitting results demonstrated a good agreement
 223 between simulation and experimental data with three correlation coefficients of R = 0.9978, 0.9973,

224 and 0.9647.

225

226 [Fig. 1]

227 [Fig. 2]

228

229 The new organic degradation model (Eq. 6) was also validated by the above first set of
230 experiments of phenol degradation at $[O_2] = 0.57$ mM, $[Fe^{2+}]_0 = 0.20$ mM and pH 2.5, but three
231 different current density ($I/A = 0.04, 0.16$ and 0.32 mA cm⁻²). The experimental data were fitted
232 using both the first-order model and our new model, respectively. Fig. 3 presents the results of
233 fittings in linear forms of the first-order model (Fig. 3A) and our new model of

234 $[Ln \frac{[S_0]}{[S]} + a([S_0] - [S])]$ vs. $(t - \frac{1 - e^{-ct}}{c})$ (Fig. 3B). It can be seen that the correlation coefficients

235 for fitting by our new model are much higher than those by the first-order model. Furthermore, Fig.

236 4 shows variation of phenol concentration $[S]$ against reaction time (t) fitted by our new model (Eq.

237 6a). The experiments demonstrated that a trend of all experimental data between phenol

238 concentration and reaction time appeared as an inverted “S” shape curve, which means that the rate

239 of phenol degradation was quite slow during the initial stage of the reaction due to a low H₂O₂

240 concentration, then significantly increased during the middle stage of the reaction due to a quick

241 growth of H₂O₂ concentration in the reaction solution, and eventually slowed down again during the

242 later stage of the reaction after phenol had been reduced to a low level. It is obvious that our new

243 model well fitted the experimental data, since the model considers both variables of phenol

244 concentration and also H₂O₂ concentration simultaneously. Actually many reactions can not be

245 simply fitted by the first-order model. Some researchers would rather subdivide the reaction period

246 into two or three phases to fit the experimental data using the first-order model separately with

247 different values of kinetic constant (k) (Chu et al., 2005). This approach may well simulate the

248 experimental data mathematically, but not chemically. Our model can satisfy the kinetic description

249 of such an E-Fenton reaction in both ways.

250

251 [Fig. 3]

252 [Fig. 4]

253

254 It has been identified that three parameters of current density (I/A), dissolved oxygen
255 concentration ($[O_2]$), and initial ferrous ion concentration $[Fe^{2+}]_0$ are the key factors affecting both
256 the H_2O_2 generation and also the phenol degradation. The experimental results shown in Fig. 4
257 demonstrated that the increase of the applied current density up to 0.32 mA cm^{-2} in the E-Fenton
258 reaction could enhance the phenol degradation significantly, since the higher rate of H_2O_2
259 generation was achieved at the higher current density. It is believed that at the lower side of current
260 density ($I/A \leq 0.32 \text{ mA cm}^{-2}$), phenol is mainly degraded by the typical E-Fenton reaction, but at the
261 higher side of current density ($I/A > 0.32 \text{ mA cm}^{-2}$), the H_2O_2 reduction to water on the cathode
262 would be involved.

263 The experimental data from the second set of experiments with different dissolved oxygen
264 concentration were fitted using the new model and the results are presented in Fig. 5. It can be seen
265 that the three curves of phenol degradation at different dissolved oxygen concentration showed the
266 same pattern of the inverted “S” shape and good fittings were achieved by our new model. Also the
267 results showed that the higher $[O_2]$ up to 0.57 mM accelerated the phenol degradation significantly,
268 but not as much as the effect of current density. These results further confirmed that the rate of
269 substance degradation can be enhanced by increasing I/A as the first-order reaction, but by
270 increasing $[O_2]$ at the order between 0 and 1 as indicated by Eq. 6. From an engineering point of
271 view, the application of such an E-Fenton reaction in water and wastewater treatment should adopt a
272 dissolved oxygen level below 9 mg l^{-1} (equivalent to 0.28 mM), which can be simply realized by
273 aeration under normal atmosphere pressure.

274

275 [Fig. 5]

276

277 It should be noted that the overall efficiency of phenol degradation in such an E-Fenton
278 reaction depends on both rates of H_2O_2 generation and Fenton reaction in the solution. When the
279 current density and dissolved oxygen concentration mainly affect the rate of H_2O_2 generation, the
280 ferrous ion concentration would affect both rates of H_2O_2 decomposition and $\cdot OH$ formation in the
281 reaction solution simultaneously. The third set of experiment of phenol degradation with different
282 initial concentrations of ferrous ion was conducted. The results presented in Fig. 6 showed that the

283 phenol degradation reaction increased with the increased initial concentrations of ferrous ion
284 ($[\text{Fe}^{2+}]_0$) from 0.05 to 0.2 mM significantly, and further enhanced from 0.2 to 1.0 mM slightly.
285 Without surprise, the inverted “S” shape curves of phenol concentration vs. reaction time were
286 confirmed and the goodness of the fittings at different $[\text{Fe}^{2+}]_0$ by our new model is presented in Fig.
287 6.

288
289 [Fig. 6]

290
291 In our study, it was further found that a turning point for the enhancement of phenol
292 degradation reaction from high to low by $[\text{Fe}^{2+}]_0$ was around 1.0 mM under our experimental
293 condition. At a higher $[\text{Fe}^{2+}]_0$ of 2.0 mM, no significant increase in phenol degradation was
294 observed. At much higher $[\text{Fe}^{2+}]_0$, the rate of phenol degradation could be reduced (not shown here).
295 These results indicate clearly that there must be an optimum ferrous ion concentration in such an
296 E-Fenton reaction. In this study, $[\text{Fe}^{2+}]_0 = 0.2$ mM was determined to be a suitable concentration to
297 achieve an efficient rate of phenol degradation under our experimental condition.

298
299 Although the conventional first-order kinetic model is the simplest model to describe a variety
300 of chemical reactions and has been widely applied in various processes relevant to water and
301 wastewater treatment, it is difficult to well describe the kinetics of the E-Fenton reaction precisely.
302 It should be noted that the cathodic E-Fenton reaction has a few particular characters that: (i) H_2O_2
303 is continuously generated throughout the reaction; (ii) the initial H_2O_2 concentration in the reaction
304 solution is zero and gradually increases along with the reaction time toward a maximum value,
305 depending on the applied current density, the dissolved oxygen concentration and the ferrous iron
306 concentration; and (iii) the variation of substrate concentration vs. reaction time has a typical
307 inverted “S” shape curve, indicating a low reaction rate during the initial stage of the reaction, a
308 high reaction rate during the middle stage, and a low reaction rate again during the final stage.

309 310 **5. Conclusion**

311
312 In this study, a new kinetic model for the E-Fenton reaction in aqueous solution was established

313 mathematically as an analytical solution by considering both the H₂O₂ generation rate and the H₂O₂
314 consumption rate. In addition, it also includes the three key factors of current density, dissolved
315 oxygen concentration and ferrous ion concentration. Therefore, this model with its inverted “S”
316 shape curve can describe the cathodic E-Fenton reaction much better than the first-order model
317 more accurately than other kinetics by subdividing the reaction period into two or three phases.
318 However, the new model was only validated by the experiments of phenol degradation so far.
319 Further studies to apply this kinetic model in degradation of other organics become necessary.

320

321 **Acknowledgements**

322 This work was financially supported by the RGC grant of Hong Kong Government (RGC Grant No.
323 PolyU5148/03E). The project is also partially supported by Natural Science Foundation of China
324 (Project No: 20577071) and Natural Science Foundation of China Guangdong Province, China
325 (Project No: 04009709). The authors would thank Mr. Zhang Guangchi for his help in the
326 modeling work.

327

328 **References**

- 329 Anota, J., Lu M.C., Chewprech, P., 2006. Kinetics of aniline degradation by Fenton and
330 electro-Fenton Processes. *Wat. Res.* 40, 1841-1847.
- 331 APHA, 1995. Standard methods for the examination of water and wastewater, 19th edition.
- 332 Boye, B., Dieng, M. M., Brillas, E., 2002. Degradation of herbicide 4-chlorophenoxyacetic acid by
333 advanced electrochemical oxidation. *Environ. Sci. Technol.* 36, 3030-3035.
- 334 Brillas, E., Baños, M. A., Garrido, J. A., 2003. Mineralization of herbicide
335 3,6-dichloro-2-methoxybenzoic acid in aqueous medium by anodic oxidation, electro-Fenton and
336 photoelectron-Fenton. *Electrochim. Acta.* 48, 1697-1705.
- 337 Brillas, E., Calpe, J. C., Casado, J., 2000. Mineralization of 2,4-D by advanced electrochemical
338 oxidation process. *Wat. Res.* 34, 2253-2262.
- 339 Brillas, E., Casado, J., 2002. Aniline degradation by Electro-Fenton[®] and peroxy-coagulation
340 processes using a flow reactor and for waste water treatment. *Chemosphere* 47, 241-248.
- 341 Brillas, E., Sauleda, R., Casado, J., 1998. Degradation of 4-chlorophenol by anodic oxidation,
342 electro-Fenton, photo-electro-Fenton and peroxi-coagulation processes. *J. Electrochem. Soc.*
343 145, 759-765.

344 Buvet, R, Sechaud, P., Darolles, J., Leport., Sechaud, F., 1987. Electrochemical and chemical
345 reductions of oxygen dissolved in aqueous solutions. *Bioelectrochem. Bioenerg.* 18, 13-19.

346 Chu W., Kwan C. Y., Chan K. H., Kam S. K., 2005. A study of kinetic modelling and reaction
347 pathway of 2,4-dichlorophenol transformation by photo-fenton-like oxidation. *J. Hazard. Mat.*
348 121, 119-126.

349 Duesterberg, C. and Waite, T. D., 2006. Process optimization of Fenton oxidation using kinetic
350 modeling. *Environ. Sci. Technol.* 40, 4189-4195

351 Gözmen, B., Oturan, M. A., Oturan, N. O., Erbatur, O., 2003. Indirect electrochemical treatment of
352 bisphenol in water via electrochemically generated Fenton reagent. *Environ. Sci. Technol.* 37,
353 3716-3723.

354 Joseph J. P., 1992. Dark and photoassisted Fe³⁺-catalyzed degradation of chlorophenoxy herbicides
355 by hydrogen peroxide. *Environ. Sci. Technol.* 26, 944-951.

356 Kawabe, S., Kaneco, S., Suzuki, T., Ohta, K., 2004. Degradation of bisphenol A in water by the
357 photo-Fenton reaction. *J. Photochem. Photobiol. A: Chem.* 162, 297-305.

358 Liu D. X., Liu J., Wen J., 1999. Elevation of hydrogen peroxide after spinal cord injury detected by
359 using the Fenton reaction. *Free Radical Biology and Medicine.* 27, 478-482.

360 Liu, H., Li, F. B., Li, X. Z., 2003. Photocatalytic oxidation using a new catalyst-titanium dioxide
361 microsphere for water and waste water treatment. *Abstr. Pap. Am Chem. S225*, PP 104.

362 Lunar, A., Sicilia, D., Rubio S., Pérez-Bendito D., Nickel, U., 2000. Degradation of photographic
363 developers by Fenton reagent: condition optimization and kinetics for metol oxidation. *Wat.*
364 *Res.*, 34, 1791-1802.

365 Malato, S., Caceres, J., Aguera, A., Mezcua, M., Hernando, D., Vial, J., Fernandez-Alba, A. R.,
366 2001. Degradation of imidacloprid in water by photo-Fenton and TiO₂ photocatalysis at a solar
367 pilot plant: A comparative study. *Environ. Sci. Technol.* 35, 4359-4366.

368 Malato, S., Caceres, J., Aguera, A., Mezcua, M., Hernando, D., Vial, J., Fernandez-Alba, A. R.,
369 2001. Degradation of imidacloprid in water by photo-Fenton and TiO₂ photocatalysis at a solar
370 pilot plant: A comparative study. *Environ. Sci. Technol.* 35, 4359-4366.

371 Neyens, E., Baeyens, J., 2003. A review of classic Fenton peroxidation as an advanced oxidation
372 technique. *J. Haz. Mat.* 98, 33-50.

373 Oliveros, E., Legrini, O., Hohl, M., Müller, T., Braun, A. M., 1997. Industrial waste water treatment:
374 large scale development of a light-enhanced Fenton reaction *Esther. Chem. Eng. Proc.* 36,
375 397-405.

376 Oturan, M. A., 2000. An ecologically effective water treatment technique using electrochemically

377 generated hydroxyl radicals for in situ destruction of organic pollutants: Application to
378 herbicide 2,4-D. *J. Appl. Electrochem.* 30, 475-482.

379 Oturan, M. A., Peiroten, J., Chartrin. P., Acher., A. J., 2000. Complete destruction of p-nitrophenol
380 in aqueous medium by electro-Fenton method. *Environ. Sci. Technol.* 34, 3474-3479.

381 Qiang, Z. M., Chang, J. H., Huang, C. P., 2002. Electrochemical generation of hydrogen peroxide
382 from dissolved oxygen in acidic solutions. *Wat. Res.* 36, 85-94.

383 Sellers, R.M., 1980. Spectrophotometric determination of hydrogen-peroxide using potassium
384 titanium(IV) oxalate. *Analyst* 105, 950-954.

385 Vogel, A., 1978. *A Textbook of Quantitative Inorganic Analysis*, fourth ed. Longman Scientific and
386 Technical, England.

387 Walling, C., 1975. Fenton Reagent Revisited. *Acc. Chem. Res.* 8, 125-131.

388 Wang, Q.Q., Lemley, A.T., 2001. Kinetic model and optimization of 2,4-D degradation by anodic
389 Fenton treatment. *Environ. Sci. Technol.* 35, 4509-4514.

390

391 **LIST OF FIGURE CAPTIONS**

392

393 Fig. 1. H₂O₂ accumulation in the reaction solution with initial phenol concentration of 1.5×10^{-4} M
394 (A) different I/A, when [O₂] = 0.57 mM and [Fe]₀ = 0.20 mM; (B) different [Fe²⁺]₀, when I/A =
395 0.32 mA cm⁻² and [O₂] = 0.57 mM; and (C) different [O₂], when I/A = 0.32 mA cm⁻² and [Fe]₀
396 = 0.20 mM.

397

398 Fig. 2. Linear fittings of [H₂O₂]_{max} at different (A): I/A, (B): [Fe²⁺]₀ and (C): [O₂], respectively.

399

400 Fig. 3. Linear relationship of phenol degradation during the E-Fenton reaction at different I/A fitted
401 by (A) the first-order model and (B) the new kinetic model, when [O₂] = 0.57 mM, [Fe]₀ = 0.2
402 mM and pH 2.5.

403

404 Fig. 4. Phenol degradation during the E-Fenton reaction at different I/A fitted by the new kinetic
405 model ([O₂] = 0.57 mM, [Fe]₀ = 0.2 mM and pH 2.5).

406

407 Fig. 5. Phenol degradation during the E-Fenton reaction at different [O₂]₀, fitted by the new kinetic
408 model ($K_{ad} = 1.1 \text{ L mM}^{-1}$, $k_1 = 6.6 \text{ M}^{-1} \text{ S}^{-1}$, $k_2 = 81 \text{ M}^{-1} \text{ S}^{-1}$, $k_5/k_3 = 0.31$, $\lambda = 0.2$, pH 2.5, I/A =
409 0.32 mA cm⁻² and [Fe²⁺]₀ = 0.2 mM).

410

411 Fig. 6. Phenol degradation during the E-Fenton reaction at different [Fe²⁺]₀ fitted by the new kinetic
412 model ($K_{ad} = 1.1 \text{ L mM}^{-1}$, $k_1 = 6.6 \text{ M}^{-1} \text{ S}^{-1}$, $k_2 = 81 \text{ M}^{-1} \text{ S}^{-1}$, $k_5/k_3 = 0.31$, $\lambda = 0.2$, pH 2.5, I/A =
413 0.32 mA cm⁻² and [O₂]₀ = 0.57 mM).

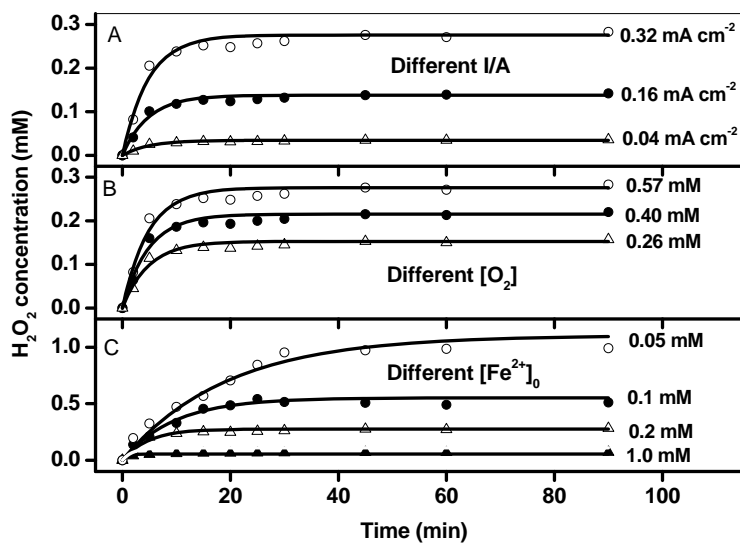


Fig. 1.

414

415

416

417

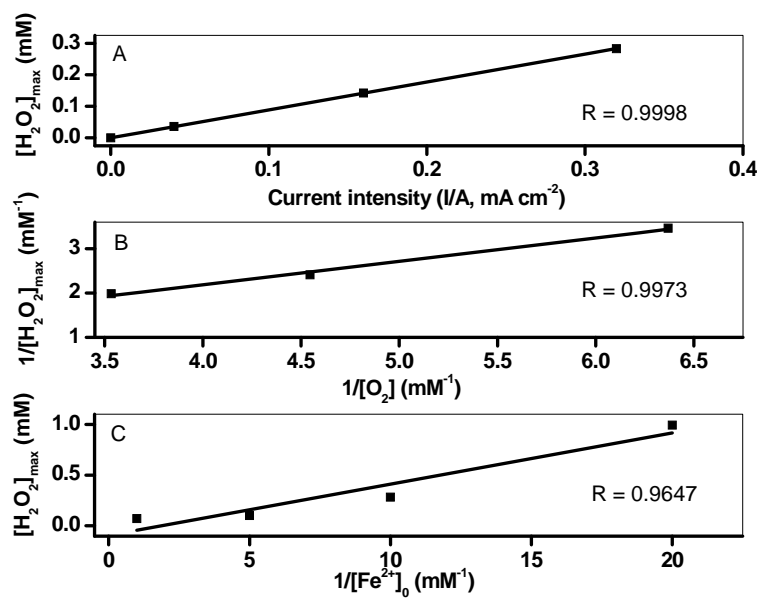
418

419

420

421

422



423

424

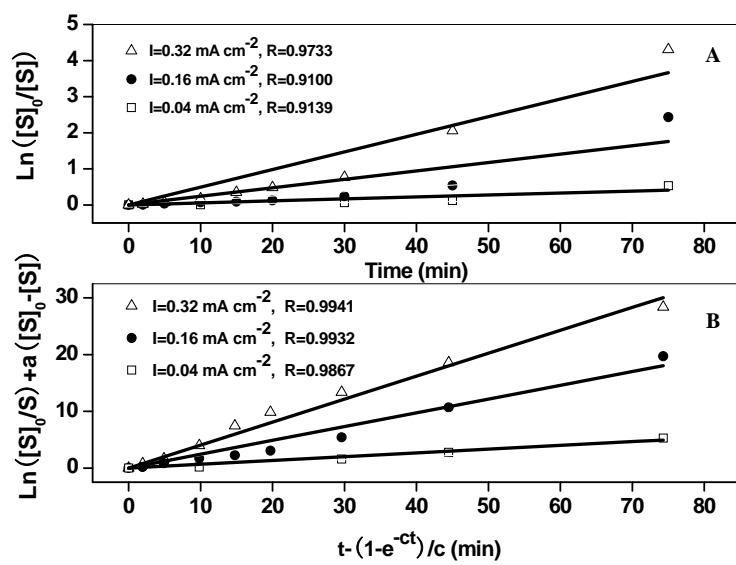
425

426

427

428

Fig. 2.



430

431

432

433

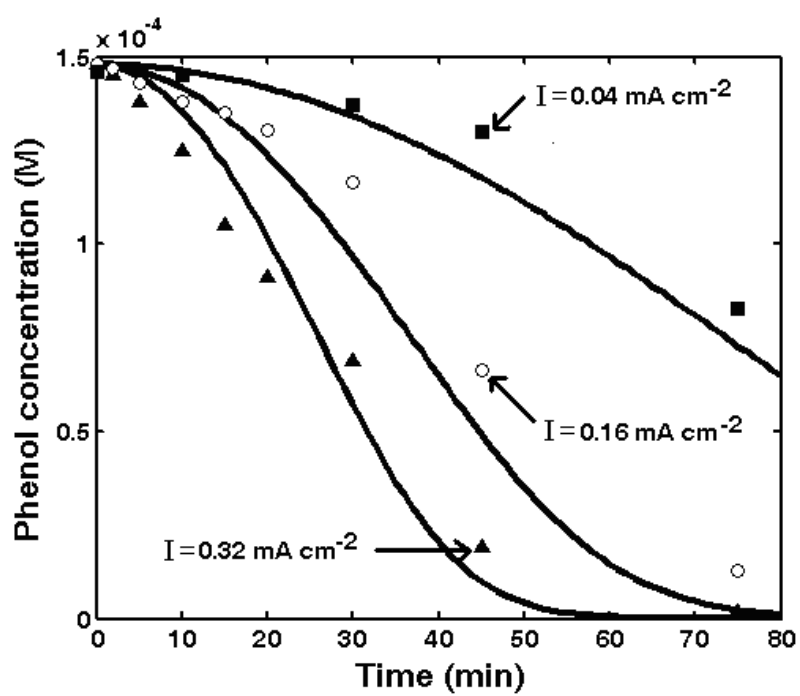
434

435

436

Fig. 3.

437



438

439

440

441

442

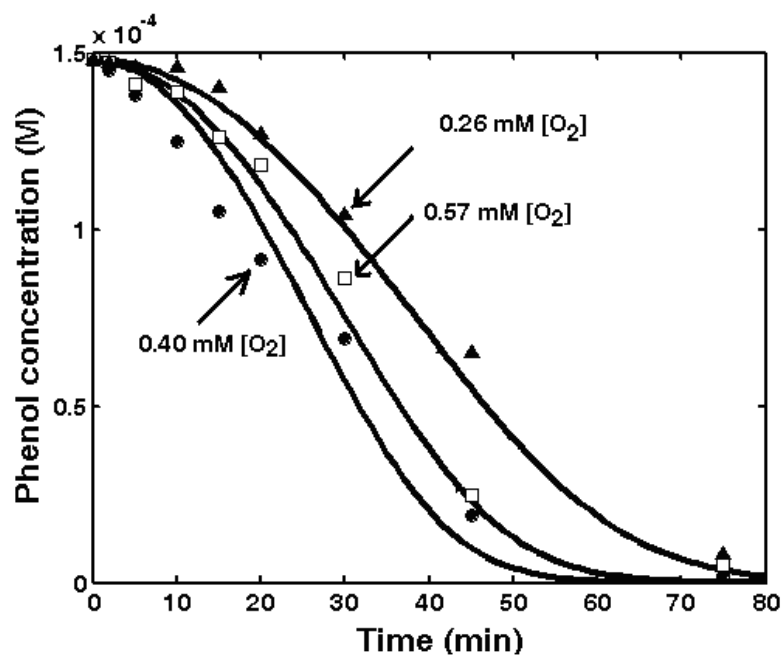
443

444

445

446

Fig. 4.



447

448

449

450

451

452

453

454

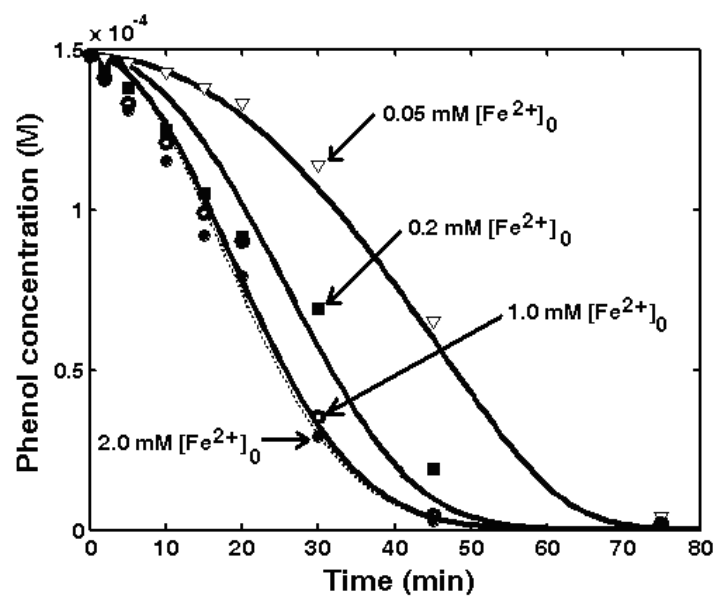
455

456

457

458

Fig. 5.



460

461

462

463

464

Fig. 6.